Periodica Polytechnica Chemical Engineering, 68(1), pp. 50–60, 2024

Pilot-scale Validation of the Modeling of NO_x Reactive Absorption Process Using Aqueous Solutions Containing Nitric Acid and Hydrogen Peroxide

Ons Ghriss[1*], Hédi Ben Amor[1], Mohamed-Razak Jeday[1], Diane Thomas[2]

[1] Processes, Energetic, Environment, and Electric Systems Laboratory, National Engineering School of Gabes (ENIG), University of Gabes, Omar Ibn. El-Khattab St., 6029 Gabes, Tunisia
[2] Chemical and Biochemical Process Engineering Unit, Faculty of Engineering (FP-UMONS), University of Mons, Place du parc 20, 7000 Mons, Belgium
[*] Corresponding author, e-mail: ons.ghriss@enig.rnu.tn

Received: 22 June 2023, Accepted: 02 November 2023, Published online: 27 February 2024

Abstract

NO_x are harmful pollutants emitted by many industries and must be removed before the gases are released into the atmosphere. Among the various techniques used for NO_x removal, reactive absorption by hydrogen peroxide in a packed column has the advantage of being able to transform NO_x into nitric acid which can be recycled and reused in the plants. This work aimed at modeling the NO_x absorption by means of aqueous solutions of hydrogen peroxide and nitric acid, applied in a packed column operating under different representative conditions. The model established using the Aspen software considers the equilibrium and the kinetics of the reactions taking place both in the gas phase and in the liquid phase as well as the thermodynamic properties of the chemical (molecular and ionic) components estimated using the Electrolyte NRTL model. It allows predicting NO_x absorption performances in terms of efficiency and selectivity. The model was validated by comparing simulation results with experimental ones obtained in a pilot-scale absorption column and published previously. The predicted values are in satisfactory agreement with the experimental data showing a deviation between 5 and 8%. Therefore, the model developed in this work could be advantageously used to design industrial-scale reactive NO_x absorption columns.

Keywords

NO_x reactive absorption, nitric acid, hydrogen peroxide, rate-based model, electrolyte NRTL model

1 Introduction

Nowadays, the unfavorable environmental and human health harms caused by emissions of NO_x [1, 2] make its reduction one of the most important challenges for industrial and scientific researchers. A variety of techniques for NO_x abatement has been developed and can be divided into two categories: dry processes and wet scrubbing processes [3, 4]. Among the dry processes can be distinguished the selective catalytic reduction (SCR), the selective non-catalytic reduction (SNCR) and the NO_x adsorption process. The selective catalytic reduction (SCR) uses ammonia or urea to promote the NO_x reduction at the surface of a catalyst conventionally based on V_2O_5-WO_3/TiO_2 or Cu- and Fe-zeolites, operating at low temperatures of 300 to 400 °C [5]. It presents certain disadvantages such as the high investment cost, the poisoning (by SO_x for example) and the limited lifetime of the catalyst, and the risk of ammonia slips [3, 6]. For its part the selective non-catalytic reduction (SNCR) using the same reagents operating under high temperature between 900 and 1000 °C [7, 8], is limited by the quite low efficiency and higher operation cost due to the higher reagent consumption [9, 10]. The NO_x adsorption process has been considered as one of the environmentally friendly technologies for the removal of NO_x. However, it presents the disadvantages of high adsorbent materials cost and a quite low efficiency [11]. On the other hand, wet scrubbing processes using water as absorbent liquid are very inefficient and strongly limited by the low solubility in water of nitric oxide NO which is usually the major constituent of NO_x species [4, 9]. To overcome this inconvenient, some reagents are added to water like sodium hypochlorite (NaClO) [12, 13], potassium permanganate [3, 14], sodium chlorite ($NaClO_2$) [6, 15, 16]

Cite this article as: Ghriss, O., Ben Amor, H., Jeday, M.-R., Thomas, D. "Pilot-scale Validation of the Modeling of NO_x Reactive Absorption Process Using Aqueous Solutions Containing Nitric Acid and Hydrogen Peroxide", Periodica Polytechnica Chemical Engineering, 68(1), pp. 50–60, 2024. https://doi.org/10.3311/PPch.22855

and hydrogen peroxide. Numerous experiments using aqueous mixtures of nitric acid and hydrogen peroxide as scrubbing solvents and applied in hollow fiber membrane modules were achieved [5] to test the NO_x reduction in gaseous effluents. Furthermore, our previous works [17] also reported that a scrubbing medium using dilute HNO_3 aqueous solutions containing H_2O_2 as oxidant is efficient for the abatement of NO_x gaseous. Experimental tests were performed in a cables-bundle contactor. In 2020, Ghriss et al. [18] present an experimental investigation of the NO_x treatment process into aqueous hydrogen peroxide solutions, with or without the presence of nitric acid, applied specifically to the flue gases issued from the nitric acid manufacturing unit of the Tunisian Chemical Group (TCG). Hydrogen peroxide has been unanimously proven to be a very attractive reagent when added in scrubbing liquors containing nitric acid as it is efficient thanks to rapid oxidation reactions involved, and results in the production of valuable nitric acid without generating liquid wastes. Table 1 [3–6, 9–11, 17, 18] lists and compares the advantages and limitations of currently used dry and wet purification methods for NO_x removal.

To apply at industrial scale the NO_x removal technology by reactive absorption using aqueous solutions containing nitric acid and hydrogen peroxide, it is necessary to have an adequate predictive model. Aspen Plus® includes tools for property methods estimation, thermodynamic calculations, and the ability to use electrolyte equilibriums and to handle chemical reactions in a wide range of unit operations. A rate-based unit operation model, in which rate-based mass and heat transfer calculations are possible, was selected in Aspen Plus®. It was used by Loutet et al. (2011) [19] for the modeling of the NO_x absorption into water and nitric acid solutions using a packed column. The built model was validated by comparison of predicted values with experimental data from industrial-scale plant in Redcar, United Kingdom. Later Laribi et al. (2019) [20] have also used Aspen Plus® simulator to model the SO_x and NO_x absorption process emitted from both power and cement oxyfuel plants operating under pressure and using water as absorbent solution and a packed column as contactor. In their model, they included a chemical reaction mechanism for the SO_x and NO_x compounds in the gas/liquid phases to evaluate the optimal conditions of the CO_2 capture process. More recently, Kurillová et al. (2019) [21] studied the modeling of the reactive absorption of nitrogen oxides generated during the production of calcium nitrate fertilizers with water as absorbent, using Aspen Plus® as a simulator. The simulation results were found to be in good agreement with the experimental data with a relative error of 5%. In their work, they propose the addition of a H_2O_2 solution into the second packed column of the calcium nitrate fertilizers process. An experimental and modeling study of desulphurization using sodium chlorite seawater solutions was presented by Flagiello et al. (2020) [22]. Aspen Plus® Process Simulation software, once properly integrated with appropriate equilibrium and mass transfer models, was used to provide a good

Table 1 Advantages and limitations of currently used purification methods for NO_x removal

Method	Advantage	Disadvantage	References
	Dry techniques		
Selective catalytic reduction (SCR)	High efficiencies	- High investment cost -Potential poisoning of catalyst - Limited lifetime of catalyst - Risk of ammonia slips	[3, 6]
Selective non-catalytic reduction (SNCR)	Acceptable investment cost	- Quite low efficiency - Higher operation cost	[9, 10]
NO_x adsorption process	Environmentally friendly technologies	- High cost of adsorbent materials - Potential degradation of adsorbent - Quite low efficiency	[11]
	Wet techniques		
Scrubbing process using water	- Not expensive. - Easily available solvent.	- Very inefficient - Strongly limited by the low solubility in water of nitric oxide	[4, 9]
Scrubbing process using dilute HNO_3 solutions containing an oxidant (H_2O_2)	- Reagent attractivity when added in scrubbing liquors containing nitric acid - Production of valuable nitric acid without generating liquid wastes, with an economical advantage for processes producing initiallyHNO$_3$ - High NO_x abatement efficiency	- High cost of H_2O_2	[5, 17, 18]

prediction of SO_2 solubility and removal efficiency data. In other works [23], a predictive mass transfer model was specifically developed, implemented in Aspen Plus® and successfully validated with desulphurization tests at different SO_2 concentrations, temperatures and for different sorbents. In [24] was reported an experimental and modeling study of the thermodynamics and kinetics of SO_2 absorption with H_2O_2 oxidative solutions.

As far as the reactive absorption of NO_x by the H_2O-HNO_3-H_2O_2 system is concerned, it was the subject of a study carried out by [25] using a pilot-scale packed column. A mathematical model based on the two-film absorption theory and considering chemical reactions and equilibrium in gas and liquid phases as well as diffusive transport, has been established, determining overall kinetic parameters for tetravalent NO_x (NO_2 and N_2O_4) and trivalent ($N_2O_3 + HNO_2$), varying with the acidity, but not reflecting the precise complex chemistry of the system. According to the bibliography listed above, the modeling of reactive NO_x absorption was mainly studied and analyzed for water or dilute nitric acid solutions but without any additional oxidizing agent. Therefore, due to the lack of modeling developments on the reactive NO_x absorption into H_2O-HNO_3-H_2O_2 system the objective of this work was to develop a numerical simulation using Aspen Plus®. The model was developed to predict NO_x absorption performances (both efficiency and selectivity) reached in an absorption column for varied operating conditions. Its validation was adequately discussed by comparing the simulated results with the 40 experimental data obtained in a pilot-scale packed column and published in earlier works.

2 Modeling and Simulation of NO_x absorption

2.1 Implementation of the absorption process

In this work, a model for NO_x absorption into the chemical system H_2O-HNO_3-H_2O_2 was developed using Aspen Plus® as process simulator. This software includes tools for property methods estimation, thermodynamic calculations, and the ability to use electrolyte equilibriums and to handle chemical reactions in a wide range of unit operations [26]. Process simulations of NO_x reactive absorption were performed using a rate-based calculation module because it considers both chemical reactions and mass (and heat) transfer in gas and liquid phases [19]. In this calculations module, the rate-based model used the correlation of Billet and Schultes (1993) [27] and the Chilton and Colburn method [28] to solve mass and heat transfers respectively. Fig. 1 presents the flowsheet of the NO_x absorption process in packed column designed in Aspen Plus®. A flue gas stream (GAS-IN) is introduced at the bottom of the absorber where it is contacted counter currently with the scrubbing solution flowing down from the top of the column (LIQ-IN). NO_x are selectively absorbed into the scrubbing solution, the rich liquid leaving at the bottom of the absorber (LIQ-OUT) and the purified gas (GAS-OUT) being released. Flow rates and compositions are given for the incoming gas and liquid, while the same variables are computed for the gas and liquid at the outlets.

2.2 Description of chemical reactions and corresponding kinetic or equilibrium data

The simulation performances are extremely dependent on the chemical mechanisms selected and, on the equilibrium, and kinetic data used. The mechanism of NO_x absorption into aqueous solutions containing H_2O_2 and HNO_3, shown in Fig. 2, has been described in several sources such as [29, 30]. The gas phase reactions are the kinetic oxidation of nitric oxide NO to nitrogen dioxide NO_2 by oxygen O_2 (R.1) and the equilibrium reactions producing dinitrogentetraoxideN_2O_4 (R.2) and dinitrogen trioxide N_2O_3 (R.3). The liquid phase reactions are considered as irreversible and kinetically controlled reactions. Via reactions (R.4) (R.5) and (R.6), N_2O_4, NO_2 and N_2O_3 compounds react rapidly with water (hydrolyses reactions) and produce nitrous and nitric acids. Nitrous acid HNO_2 is unstable and can decompose with the release of NO while nitric acid is stable in the liquid phase. It is reported that the presence of H_2O_2 in the liquid phase improves NO_x absorption by oxidation of HNO_2 [31, 32] and of NO [33] into HNO_3 according to reactions (R.7) and (R.8), respectively known to be fast and irreversible. It was shown that the presence of nitric acid promotes the oxidation reaction of HNO_2 (R.7) thanks to an auto-catalytic effect [29]. Characteristics of the reactions included in the model are given in Table 2 [30, 32–37].

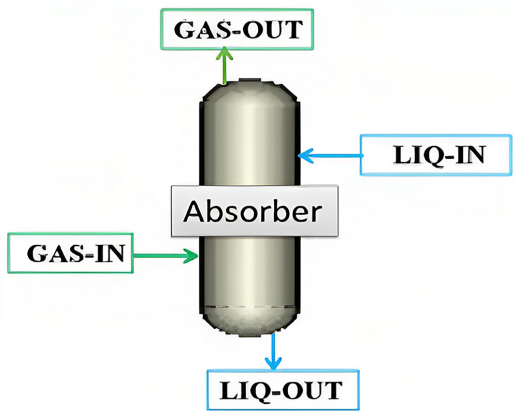

Fig. 1 Aspen Plus® flow-sheet for NO_x reactive absorption column

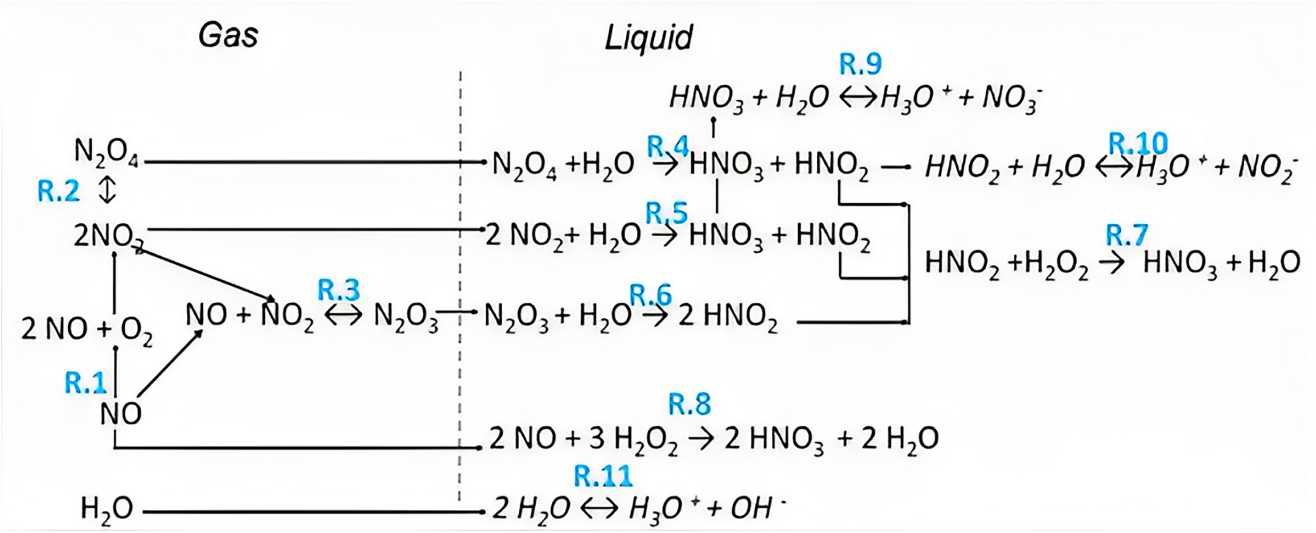

Fig. 2 Absorption mechanisms of NO_x into aqueous solutions containing H_2O_2 and HNO_3 used in the model (adapted from [30])

Table 2 Characteristics of the reactions included in the model

Reaction	Equilibrium constants, kinetic constants and reaction rate expression	Sources
	Gaseous phase	
$2NO + O_2 \xrightarrow{R.1} 2NO_2$	$r_{NO}^G = k_{NO}^G C_{NO}^2 C_{O_2}$ $k_{NO}^G = 970\exp(5003/RT)$ $k_{NO}^G(293\ \text{K}) = 7571\ (\text{m}^6/\text{kmol}^2\ \text{s})$	[34]
$2NO_2 \xleftrightarrow{R.2} N_2O_4$	$K_{N_2O_4}^G = P_{N_2O_4}/P_{NO_2}^2 = 5.6910^{-15}\exp(6891.6/T)$ $K_{N_2O_4}^G(293\ \text{K}) = 9.3310^{-5}\ (1/\text{Pa})$	[35]
$NO + NO_2 \xleftrightarrow{R.3} N_2O_3$	$K_{N_2O_3}^G = P_{N_2O_3}/P_{NO_2}P_{NO} = 6.4110^{-13}\exp(4740/T)$ $K_{N_2O_3}^G(293\ \text{K}) = 6.8010^{-6}\ (1/\text{Pa})$	[30]
	Liquid phase	
$2NO_2 + H_2O \xrightarrow{R.4} HNO_3 + HNO_2$	$r_{NO_2}^L = k_{NO_2}^L C_{NO_2}^2$ $k_{NO_2}^L = 2994.65\exp(23714/RT)$ $k_{NO_2}^L(293\ \text{K}) = 5.0810^7\ (\text{m}^3/\text{kmol s})$	[36]
$N_2O_4 + H_2O \xrightarrow{R.5} HNO_3 + HNO_2$	$r_{N_2O_4}^L = k_{N_2O_4}^L C_{N_2O_4}$ $k_{N_2O_4}^L(293\ \text{K}) = 670\ (1/\text{s})$	[30]
$N_2O_3 + H_2O \xrightarrow{R.6} 2HNO_2$	$r_{N_2O_3}^L = k_{N_2O_3}^L C_{N_2O_3}$ $k_{N_2O_3}^L(293\ \text{K}) = 1.210^4\ (1/\text{s})$	[37]
$HNO_2 + H_2O_2 \xrightarrow{R.7} HNO_3 + H_2O$	$r_{HNO_2}^L = k_{HNO_2}^L C_{H_3O^+} C_{H_2O_2} C_{HNO_2}$ $k_{HNO_2}^L = 3.510^{13}\exp(-55549/RT)$ $k_{HNO_2}^L(293\ \text{K}) = 4.310^3\ (\text{m}^6/\text{kmol s})$	[32]
$2NO + 3H_2O_2 \xrightarrow{R.8} 2HNO_3 + 2H_2O$	$r_{NO}^L = k_{NO}^L C_{H_2O_2} C_{NO}$ $k_{NO}^L = 1.05210^{13}\exp(-58573/RT)$ $k_{NO}^L(293\ \text{K}) = 3.7510^2\ (\text{m}^3/\text{kmol s})$	[33]
$HNO_3 + H_2O \xleftrightarrow{R.9} H_3O^+ + NO_{3^-}$	$k_{HNO_3}^L(293\ \text{K}) = 3.147\ (\text{kmol}/\text{m}^3)$	Aspen Plus® database
$HNO_2 + H_2O \xleftrightarrow{R.10} H_3O^+ + NO_{2^-}$	$k_{HNO_2}^L(293\ \text{K}) = 5.18810^{-4}\ (\text{kmol}/\text{m}^3)$	Aspen Plus® database
$2H_2O \xleftrightarrow{R.11} H_3O^+ + OH^-$	$k_{H_2O}^L(293\ \text{K}) = 10^{-14.17}\ (\text{kmol}^2/\text{m}^6)$	Aspen Plus® database

Superscripts: G: gas phase, L: liquid phase

2.3 Selection of thermodynamic model for the liquid phase

In addition to reactions R.1 to R.8, three electrolyte dissociation reactions (R.9)–(R.11) giving ionic species are taken into consideration in our absorption system and are shown also in Fig. 2. Equilibrium constants for these reactions are available in Aspen Plus® Database. The Electrolyte Non-Random Two Liquid (NRTL) property method in Aspen Plus® was selected for thermodynamic properties estimations as the recommended option for systems containing electrolytes because of ionic interactions in the liquid phase requiring the use of an electrolytic equation of state. Its compatibility with the system NO_x-HNO_3-H_2O_2 for both the liquid and gas phases was tested successfully by [38]. The properties of the liquid phase are assessed from an activity-coefficient model based on the NRTL equations and the properties of the vapor phase from the Redlich-Kwong equation of state [19, 39].

3 Application of experimental results at the pilot scale

3.1 Design and operating conditions

NO_x removal efficiencies were obtained from absorption tests achieved in a pilot packed column where the gas enters axially at the bottom of the column while the fresh scrubbing solution is fed at the top with a continuous countercurrent contact. The gaseous mixture, made of air and NO_x, was analyzed at the inlet and outlet of the absorber by chemiluminescence. This technique gives the total NO_x and the chemical NO (noticed NO^*), representing the low oxidation state NO_x species given by chemiluminescence (sum of bivalent species and half of trivalent species).

$$P_{NO^*} = P_{NO} + P_{N_2O_3} \tag{1}$$

The partial pressures of NO_2^*, the chemical NO_2 (high oxidation state NO_x species, representing the sum of tetravalent species and half of trivalent species) and of total NO_x can be defined as follows:

$$P_{NO_2^*} = P_{NO_2} + 2P_{N_2O_4} + P_{N_2O_3} \tag{2}$$

$$P_{NO_x} = P_{NO_2^*} + P_{NO^*}\,. \tag{3}$$

The oxidation ratio OR in the gas phase is an important characteristic of the gas and is defined by

$$\mathrm{OR} = \frac{P^{in}_{NO_x} - P^{in}_{NO^*}}{P^{in}_{NO_x}}\,. \tag{4}$$

As far as the pilot-scale absorber is concerned the characteristic design parameters are depicted in Table 3.

A screening series of continuous absorption tests was conducted at 293 K with a given gas flow rate but varying liquid flow rates and liquid phase compositions according to values in Table 4.

Each absorption experiment was evaluated by a quantitative performance, the overall NO_x absorption efficiency (A_{NO_x}) and by a qualitative one, the absorption selectivity of tetravalent nitrogen oxides ($S_{NO_2^*}$) with these definitions:

$$A_{NO_x}(\%) = 100\left[\frac{P^{in}_{NO_x} - P^{out}_{NO_x}}{P^{in}_{NO_x}}\right] \tag{5}$$

$$S_{NO_2^*}(\%) = 100\left[\frac{P^{in}_{NO_2^*} - P^{out}_{NO_2^*}}{P^{in}_{NO_x} - P^{out}_{NO_x}}\right], \tag{6}$$

where "in" means inlet and "out" means outlet. Further details on the experimental set-up and procedure are given by [40].

3.2 Definition and distribution of NO_x species in the gaseous phase

Aspen Plus® simulator requires the partial pressures of the different NO_x species (NO, NO_2, N_2O_3 and N_2O_4) present in the inlet gas to estimate their individual absorption fluxes. These can be calculated from P_{NO_x} and OR values (or P_{NO^*} and $P_{NO_2^*}$) according to the following approach, taking into account that the various nitrogen oxides are

Table 3 Main characteristics of the pilot-scale absorber

Packing type	Pall rings
Material	Polypropylene
Packing size (m)	0.025
Void fraction (%)	91
Specific surface area (m^2/m^3)	220
Packed height (m)	2.14

Table 4 Operating conditions for the pilot-scale column

Variables	Value
L	$1.111 \times 10^{-4} - 1.944 \times 10^{-4}$ m^3/s
G	0.0355 m^3/s
Gas phase composition	Molar/volume fractions: NO_x: $665 \times 10^{-6} - 4168 \times 10^{-6}$ O_2: 0.20 N_2: 0.77 H_2O: 0.023
OR	50–98%
Liquid phase composition	HNO_3: 0–1 M H_2O_2: 0.2 M

Abbreviations: G: Volumetric gas flow rate (m^3/s),
L: Volumetric liquid flow rate (m^3/s)

in equilibrium in the gas phase according to reactions R.2 and R.3 whose constant values are given in Table 2:

$$P_{NO_2^*} - P_{NO^*} = P_{NO_2} + 2K^G_{N_2O_4} P^2_{NO_2} - P_{NO} \quad (7)$$

and

$$P_{NO_x} = P_{NO}\left(1 + 2K^G_{N_2O_3} P_{NO_2}\right) + P_{NO_2}\left(1 + 2K^G_{N_2O_4}\right). \quad (8)$$

The distribution of the different NO_x species can be then determined by an iterative resolution. The obtained results were regrouped in Table 5 by considering the operating P_{NO_x} and OR values specific to the 40 experimental data published by [40]. Fig. 3 gives the evolution of the distribution of the partial pressures of the various species versus the NO_x oxidation ratio at T = 293 K, expressed on logarithmic scale, for values of P_{NO_x} = 105.9 Pa and P_{NO_x} = 398.5 Pa.

According to Fig. 3, whatever the NO_x partial pressure, it is found that the N_2O_3 species is in low proportion in comparison with other species and reaches a maximum partial pressure for an oxidation ratio of about 50%. The partial pressure of N_2O_4 increases with OR similarly to that of the NO_2 species, whereas the partial pressure of NO decreases when OR is increasing. Nevertheless, it was clearly shown in the literature [40] that due to their very high solubility and reactivity properties the N_2O_3 and N_2O_4 species, with low concentrations but rapidly produced (by equilibrium reactions), take part substantially in the overall NO_x absorption mechanism.

4 Model results and validation

To check the validity of the model developed, a comparison of the results predicted by the Aspen rate-based model and the experimental data taken from the literature [38] is performed, by varying the solvents tested, the liquid flow rate, the NO_x partial pressure and the oxidation ratio. The input data, operating conditions and absorption results of the 40 experimental pilot-scale tests are summarized in Table 5.

For each absorption test, from the inlet gas composition, whose speciation (NO, NO_2, N_2O_3, and N_2O_4) is determined as discussed previously, the model allows to calculate successively for the different NO_x species the absorbed quantities and the partial pressures in the outlet gas. Therefore, the NO_x absorption efficiency ($A_{NO_x,mod}$) and the NO_2^* absorption selectively ($S_{NO_2^*,mod}$) can be obtained according to expressions 18 and 19. Model results and experimental results for A_{NO_x} and $S_{NO_2^*}$ are presented in Fig. 4 through parity plots. The average deviation between experimental and calculated values of A_{NO_x} and $S_{NO_2^*}$ was determined using Eq. (9) given by [40].

In fact, since the absorption efficiency and selectivity play similarly important roles in characterizing the absorption performances of chemical NO and NO_2, which reflects respectively the complementary aspects of quantity and quality of NO_x absorbed, the same weightings were given to both parameters in the deviation definition:

$$\frac{1}{n_e}\sum_{i=1}^{n_e}\left(0.5\left|\left(A_{NO_x,exp}\right)_i - \left(A_{NO_x,mod}\right)_i\right| + 0.5\left|\left(S_{NO_2^*,exp}\right)_i - \left(S_{NO_2^*,mod}\right)_i\right|\right). \quad (9)$$

From the results shown in Fig. 4, it can be observed that the model built predicts the experimental results within an accuracy of 5% for Water + H_2O_2 and for HNO_3 0.5 M + H_2O_2, and of 8% for HNO_3 1 M + H_2O_2. The rate-base model here developed is thus quite satisfactorily validated for the given set of experimental results. The effect of nitric acid with concentration varied from 0 to 1 M into aqueous solution of H_2O_2 (0.02 M) was studied and presented in Fig. 5. As clearly given by Fig. 5, A_{NO_x} increases when nitric acid is gradually added to the hydrogen solution. This result is attributed to the fact that the oxidation reaction of HNO_2 is enhanced by the auto-catalytic effect of H^+ and particularly visible for intermediate oxidation ratios [29].

Table 5 Operating conditions, gas phase compositions and experimental absorption performances

		Input data			Calculated distribution of the different NO_x species				Experimental absorption performances	
Run (i)	Solvent	$L \times 10^{-4}$ ($m^3\ s^{-1}$)	P_{NO_x} (Pa)	OR (%)	P_{NO_2} (Pa)	P_{NO} (Pa)	$P_{N_2O_3}$ (Pa)	$P_{N_2O_4}$ (Pa)	$A_{NO_x,exp}$ (%)	$S_{NO_2^*,exp}$ (%)
1	Water + H_2O_2 0.2 M	1.111	66.5	98	64.30	1.32	0.00058	0.43	15.8	98
2		1.111	105.9	97	100.59	3.17	0.00219	1.06	18.1	97.4
3		1.389	124.7	96.7	117.67	4.11	0.00332	1.45	16.5	92.7
4		1,.389	250	95.4	227.62	11.49	0.01796	5.43	25.7	93.6
5		1.667	398.5	94.1	349.35	23.48	0.05636	12.80	36.9	93.2
6		1.667	72.7	82.4	59.16	12.79	0.00519	0.36	8	75.9
7		1.944	99.4	74.7	73.12	25.14	0.01263	0.56	8	51.3
8		1.944	87.8	59.8	51.93	35.28	0.01259	0.28	5.1	67.7
9		1.944	270	52.5	137.71	128.18	0.12127	1.98	17.5	65.2
10		1.944	218	57.1	121.34	93.48	0.07793	1.54	15.3	65.2
11		1.944	295	55.9	159.49	130.02	0.14247	2.66	20.7	80
12		1.944	104.5	76.9	79.04	24.13	0.01310	0.65	13.8	86.8
13		1.944	151.6	54.9	81.80	68.35	0.03841	0.70	13.5	68.3
14	HNO_3 0.5 M + H_2O_2 0.2 M	1.111	74.6	96.9	71.22	2.31	0.00113	0.53	9.6	88.6
15		1.111	231.3	94.8	210.015	12.01	0.01734	4.62	25.5	90.8
16		1.389	373.7	94.3	329.58	21.27	0.04817	11.39	32.8	92.3
17		1.389	113.7	96.2	106.97	4.31	0.00317	1.20	11.4	88.5
18		1.389	196.5	95.3	180.42	9.22	0.01144	3.41	23.5	91.5
19		1.389	320.7	94.8	286.75	16.65	0.03282	8.62	33.1	92.8
20		1.667	91.3	85.2	76.55	13.50	0.00710	0.61	9.7	71.4
21		1.667	153.6	81.4	121.90	28.55	0.02391	1.55	18.9	77.6
22		1.667	193.3	68.7	129.26	60.47	0.05370	1.75	22.7	68.2
23		1.944	306.5	64	188.62	110.26	0.14289	3.73	27.9	59.9
24		1.944	220.7	54.7	117.77	99.93	0.08085	1.45	19.9	55.6
25	HNO_3 1 M + H_2O_2 0.2 M	1.111	90.4	96.7	85.86	2.98	0.00175	0.77	7.7	87.1
26		1.111	227.4	95.3	207.65	10.68	0.01523	4.52	24	91.9
27		1.111	416.8	94.8	366.86	21.64	0.05455	14.11	39.6	90.9
28		1.389	340.1	94.9	303.42	17.32	0.03611	9.65	32.9	92.8
29		1.389	109.3	83.8	89.89	17.70	0.01093	0.84	7.9	42.1
30		1.389	183.4	85.1	151.25	27.31	0.02838	2.40	23.1	80.4
31		1.389	280.2	79.3	212.66	57.95	0.08467	4.74	30.4	75.9
32		1.667	268.2	63.6	164.82	97.56	0.11047	2.84	24.3	64
33		1.667	343	70	229.01	102.81	0.16176	5.50	32.2	72.5
34		1.667	218.3	95.9	200.87	8.94	0.01234	4.23	24.4	92.4
35		1.667	237.1	56.3	129.90	103.56	0.09242	1.77	21.7	54.9
36		1.667	342.7	73.6	240.06	90.39	0.14908	6.042	37.4	77.4
37		1.944	241.4	94.8	218.79	12.54	0.01885	5.02	38.6	77.4
38		1.944	191.3	82.5	152.90	33.45	0.03514	2.45	21.3	76
39		1.944	118.3	81.1	94.07	22.35	0.01444	0.92	12.8	70.7
40		1.944	53.6	74.8	39.75	13.50	0.00368	0.16	10.4	58.9

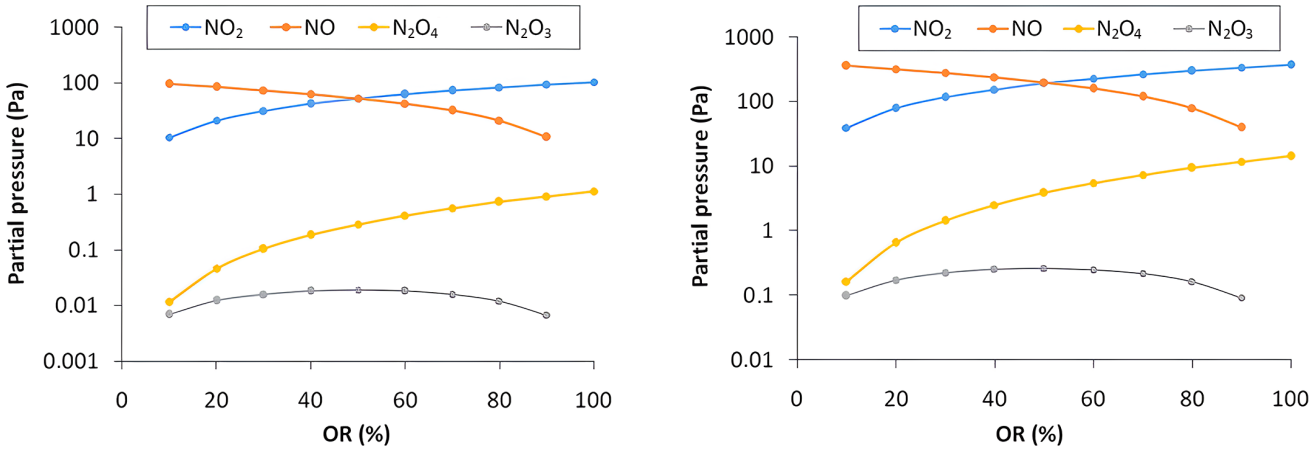

(a) (b)

Fig. 3 Equilibrium between nitrogen oxides versus the NO_x oxidation ratio at $T = 293$ K for: (a) $P_{NO_x} = 105.9$ Pa; (b) $P_{NO_x} = 398.5$ Pa

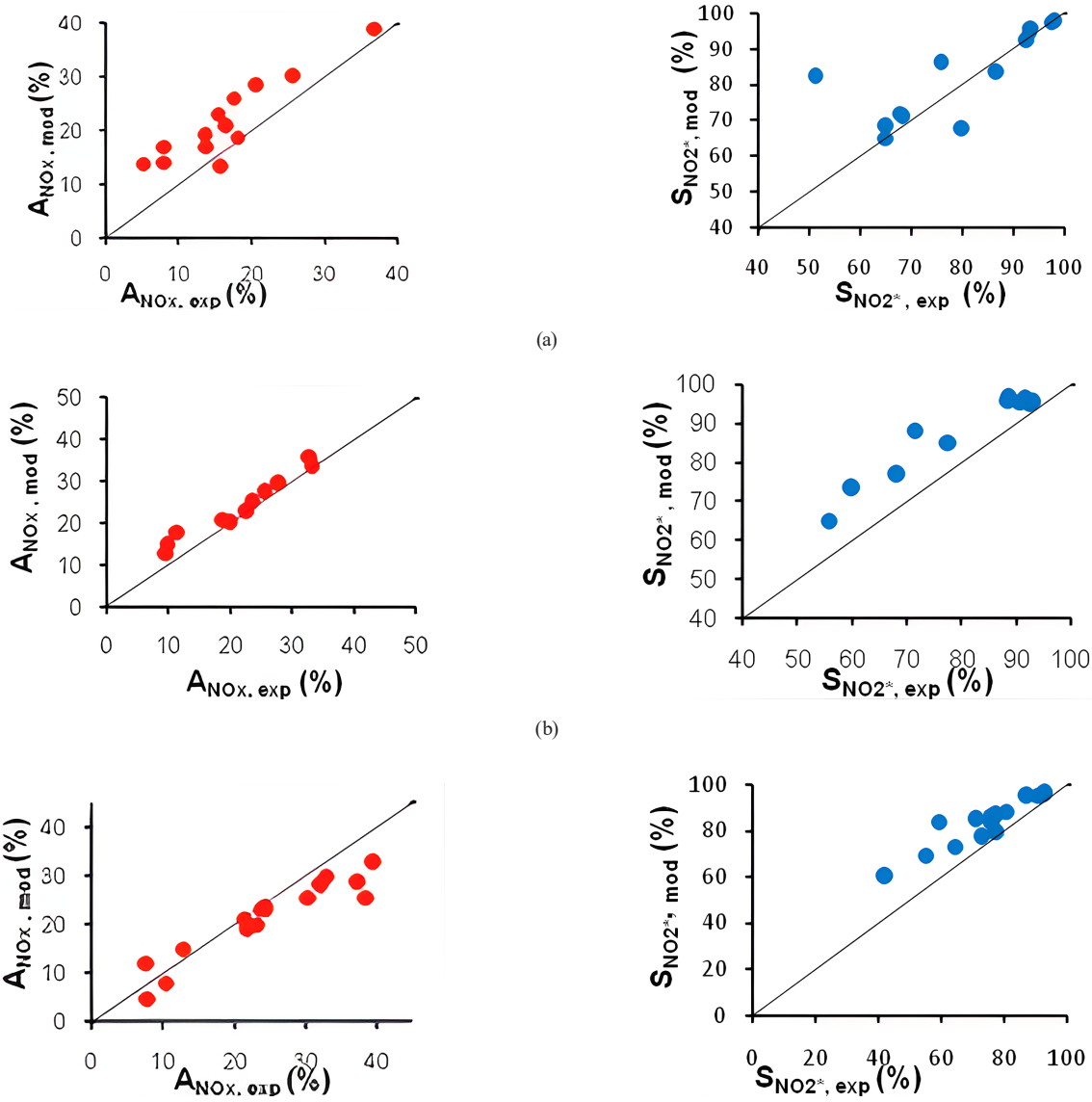

(a)

(b)

(c)

Fig. 4 Comparison between model and experimental results (NO_x absorption efficiency (left) and selectivity (right)) for: (a) water + H_2O_2 0.2 M, (b) HNO_3 0.5 M + H_2O_2 0.2 M, (c) HNO_3 1 M + H_2O_2 0.2 M

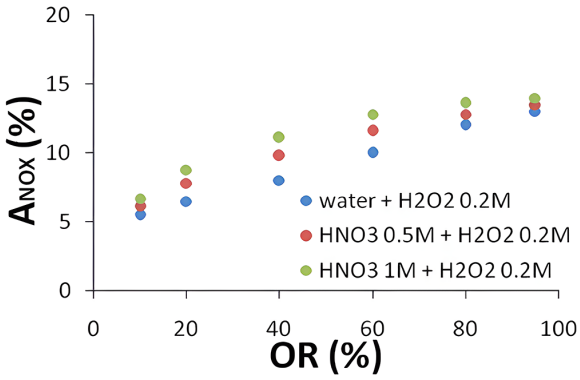

Fig. 5 Effect of the initial concentration of HNO_3, in presence of H_2O_2, at various OR values on A_{NO_x} for $P = 300$ Pa

5 Conclusion

In this work simulation results were presented using a rate-based model for NO_x reactive absorption process carried out in a pilot-scale packed column with aqueous solutions containing nitric acid and hydrogen peroxide. 40 experimental tests in total were simulated using Aspen Plus® process simulator. To apply the rate-based model, calculations of various NO_x species in the gaseous phase were carried out based on literature data. The simulation results have shown that the NO_x absorption efficiency and selectivity can be predicted with quite satisfactory low deviations from the experimental data for the different scrubbing solutions investigated, when varying several operating conditions such as the liquid flow rate, the HNO_3 concentration, the NO_x partial pressure and the oxidation ratio in the gas phase. The average deviation between experimental and calculated values of A_{NO_x} and $S_{NO_2^*}$ was around 5% for water + H_2O_2 and HNO_3 0.5 M + H_2O_2, and 8% for HNO_3 1 M + H_2O_2. Our parametric analysis has also shown how the change in NO_x partial pressure and composition (oxidation ratio) influence both the NO_x absorption efficiency (A_{NO_x}) and the NO_2^* absorption selectively ($S_{NO_2^*}$). In for all values of P_{NO_x}, the performances A_{NO_x} and $S_{NO_2^*}$ increase when OR increases. A_{NO_x} increases with HNO_3 concentrations as H^+ ions enable to catalyze the oxidation reaction of HNO_2 by H_2O_2 in the liquid phase. The applicability of the model is then assessed in the operating range of HNO_3 (0–1 M) and H_2O_2 (0.2 M) concentrations and of NO_x partial pressures (~50 Pa–500 Pa) investigated to design in the future a new full-scale oxidative scrubbing system for deNO_x, applied, as an interesting case study, to tail gases issued from a Tunisian nitric acid plant.

Abbreviations

A_{NO_x}: NO_x absorption efficiency (%);
C: Concentration in the aqueous phase (kmol/m^3);
G: Volumetric gas flow rate (m^3/s);
K: Equilibrium constant of gaseous formation;
k: Reaction rate constant for a phase reaction
L: Volumetric liquid flow rate (m^3/s);
n_e: Number of experiments;
OR: Oxidation ratio (%);
P: Partial pressure (Pa);
r: kinetic rate (kmol/m^3 s);
$S_{NO_2^*}$: tetravalent NO_x absorption selectivity (%);
T: temperature (K)

Subcripts/superscripts

exp: experimental value
G: gas phase
in: inlet
L: liquid phase
mod: calculated value
out: outlet

Conflicts of interests

This work has not been published previously; it is not under consideration for publication elsewhere.

Its publication is approved by all others. If accepted it will not be published elsewhere.

References

[1] Park, J.-H., Ahn, J.-W., Kim, K. H., Son, Y.-S. "Historic and Futuristic Review of Electron Beam Technology for the Treatment of SO_2 and NOx in Flue Gas", Chemical Engineering Journal, 335, pp. 351–366, 2019. https://doi.org/10.1016/j.cej.2018.08.103

[2] Lasne, J., Lostier, A., Salameh, T., Athanasopoulou, E., Karagiannis, D., Kakouri, A ., Vassaux, S., Lesueur, D., Romanias, M. N. "NOx emissions by real-world fresh and old asphalt mixtures: Impact of temperature, relative humidity, and UV-irradiation", Urban Climate, 49, 101457, 2023. https://doi.org/10.1016/j.uclim.2023.101457

[3] Cai, Y., Yong, L., Chu, G.-W., Wu, W., Yu, X., Sun, B.-C., Chen, J.-F. "NO_x removal in a rotating packed bed: Oxidation and enhanced absorption process optimization", Separation and Purification Technology, 227, 115682, 2019. https://doi.org/10.1016/j.seppur.2019.115682

[4] Jiang, K., Yu, H., Chen, L., Fang, M., Azzi, M., Cottrell, A., Li, K. "An advanced, ammonia-based combined $NO_x/SO_x/CO_2$ emission control process towards a low-cost, clean coal technology", Applied Energy, 260, 114316, 2020. https://doi.org/10.1016/j.apenergy.2019.114316

[5] Kartohardjono, S., Merry, C., Rizky, M. S., Pratita, C. C. "Nitrogen oxide reduction through absorbent solutions containing nitric acid and hydrogen peroxide in hollow fiber membrane modules", Heliyon, 5(12), e02987, 2019.
https://doi.org/10.1016/j.heliyon.2019.e02987

[6] Flagiello, D., Erto, A., Lancia, A., Di Natale, F. "Advanced exhaust-gas scrubbing for simultaneous de-SO_x/NO_x using a wet oxidative process with integrated washwater treatment", Chemical Engineering Research and Design, 194, pp. 731–741, 2023.
https://doi.org/10.1016/j.cherd.2023.05.014

[7] Shin, J. K., Jo, S.-H., Kim, T.-H., Oh, Y.-H., Yu, S., Son, Y.-S., Kim, T.-H. "Removal of NO_x using electron beam process with NaOH spraying", Nuclear Engineering and Technology, 54(2), pp. 486–492, 2022.
https://doi.org/10.1016/j.net.2021.06.033

[8] Zhu, Z., Xu, B. "Purification Technologies for NOx Removal from Flue Gas: A Review", Separations, 9(10), 307, 2022.
https://doi.org/10.3390/separations9100307

[9] Si, T., Wang, C., Yan, X., Zhang, Y., Ren, Y., Hu, J., Anthony, E. J. "Simultaneous removal of SO_2 and NOx by a new combined spray-andscattered-bubble technology based on preozonation: From lab scale to pilot scale", Applied Energy, 242, pp. 1528–1538, 2019.
https://doi.org/10.1016/j.apenergy.2019.03.186

[10] Li, W., Shi, X., Zhang, S., Qi, G. "Modelling of ammonia recovery from wastewater by air stripping in rotating packed beds", Science of The Total Environment, 702, 134971, 2020.
https://doi.org/10.1016/j.scitotenv.2019.134971

[11] Zhu, H., Song, S., Wang, R. "Removal of NOx by Adsorption/Decomposition on H3PW12O40·6H2O Supported on Ceria", Aerosol and Air Quality Research, 20(10), pp. 2273–2279, 2020.
https://doi.org/10.4209/aaqr.2020.03.0110

[12] Sun, W.-Y., Ding, S.-L., Zeng, S.-S., Su, S.-J., Jiang, W.-J. "Simultaneous absorption of NO_x and SO_2 from flue gas with pyrolusite slurry combined with gas-phase oxidation of NO using ozone", Journal of Hazardous Materials, 192(1), pp. 124–130, 2011.
https://doi.org/10.1016/j.jhazmat.2011.04.104

[13] Byoun, S., Shin, D. N., Moon, I.-S., Byun, Y. "Quick vaporization of sprayed sodium hypochlorite ($NaClO_{(aq)}$) for simultaneous removal of nitrogen oxides (NO_x), sulfur dioxide (SO_2), and mercury (Hg^0)", Journal of the Air & Waste Management Association, 69(7), pp. 857–866, 2019.
https://doi.org/10.1080/10962247.2018.1556187

[14] Hu, J. J., Liu, J., Zheng, Y., Cen, C, P., Gan, F. X. "A Study on the Removal of NO_x in Simulated Flue Gas Using Urea/Potassium Permanganate Solution as Absorbent", Applied Mechanics and Materials, 71–78, pp. 2797–2805, 2011.
https://doi.org/10.4028/www.scientific.net/AMM.71-78.2797

[15] Zhao, Y., Guo, T.-X., Chen, Z.-Y., Du, Y.-R. "Simultaneous removal of SO_2 and NO using M/ $NaClO_2$ complex absorbent", Chemical Engineering Journal, 160(1), pp. 42–47, 2010.
https://doi.org/10.1016/j.cej.2010.02.060

[16] Zhou, Y., Zhang, J., Baral, A., Ju, S., Gu, Y. "High-efficiency absorption of low NO_X concentration in metallurgical flue gas using a three dimensional printed large-flow microstructured reactor", Arabian Journal of Chemistry, 15(4), 103711, 2022.
https://doi.org/10.1016/j.arabjc.2022.103711

[17] Ghriss, O., Ben Amor, H., Jeday, M.-R., Thomas, D. "Nitrogen oxides absorption into aqueous nitric acid solutions containing hydrogen peroxide tested using a cables-bundle contactor", Atmospheric Pollution Research, 10(1), pp. 180–186, 2019.
https://doi.org/10.1016/j.apr.2018.07.007

[18] Ghriss, O., Ben Amor, H., Chekir, H., Jeday, M.-R. "NO_x scrubbing with H_2O_2/HNO_3 solutions achieved with a laboratory bubble contactor", Journal of Material Cycles and Waste Management, 22(1), pp. 56–64, 2020.
https://doi.org/10.1007/s10163-019-00912-7

[19] Loutet, K. G., Mahecha-Botero, A., Boyd, T., Buchi, S., Reid, D., Brereton, C. M. H. "Experimental Measurements and Mass Transfer/Reaction Modeling for an Industrial NO_x Absorption Process", Industrial & Engineering Chemistry Research, 50(4), pp. 2192–2203, 2011.
https://doi.org/10.1021/ie100436p

[20] Laribi, S., Dubois, L., Duprez, M. E., De Weireld, G., Thomas, D. "Simulation of the Sour-Compression Unit (SCU) process for CO_2 purification applied to fue gases coming from oxy-combustion cement industries", Computers & Chemical Engineering, 121, pp. 523–539, 2019.
https://doi.org/10.1016/j.compchemeng.2018.11.010

[21] Kurillová, E., Gazdová, K., Variny, M., Fecko, P. "Efficiency Improvement in Reactive Absorption of Nitrogen Oxides", Environmental Engineering Science, 36(11), pp. 1433–1442, 2019.
https://doi.org/10.1089/ees.2019.0086

[22] Flagiello, D., Di Natale, F., Erto, A., Lancia, A. "Wet oxidation scrubbing (WOS) for flue-gas desulphurization using sodium chlorite seawater solutions", Fuel, 277, 18805, 2020.
https://doi.org/10.1016/j.fuel.2020.118055

[23] Flagiello, D., Di Natale, F., Lancia, A., Erto, A. "Characterization of mass transfer coefficients and pressure drops for packed towers with Mellapak 250.X", Chemical Engineering Research and Design, 161, pp. 340–356, 2020.
https://doi.org/10.1016/j.cherd.2020.06.031

[24] Flagiello, D., Di Natale, F., Lancia, A., Sebastiani, I., Navab, F., Milicia, A., Erto, A. "Experimental and modelling approach to the design of chemical absorption columns with fast gas-liquid reaction: A case-study on flue-gas desulfurization with H_2O_2 oxidative solutions", Chemical Engineering Research and Design, 194, pp. 425–438, 2023.
https://doi.org/10.1016/j.cherd.2023.04.040

[25] Thomas, D., Vanderschuren, J. "Modeling of NO_x Absorption into Nitric Acid Solutions Containing Hydrogen Peroxide", Industrial & Engineering Chemistry Research, 36(8), pp. 3315–3322, 1997.
https://doi.org/10.1021/ie960436g

[26] Sanchez, M., Amores, E., Abad, D., Rodriguez, L., Clemente-Jul, C. "Aspen Plus model of an alkaline electrolysis system for hydrogen production", International Journal of Hydrogen Energy, 45(7), pp. 3916–3929, 2019.
https://doi.org/10.1016/j.ijhydene.2019.12.027

[27] Billet, R., Schultes, M. "Predicting mass transfer in packed columns", Chemical Engineering & Technology, 16(1), pp. 1–9, 1993.
https://doi.org/10.1002/ceat.270160102

[28] Chilton, T. H., Colburn, A. P. "Mass Transfer (Absorption) Coefficients Prediction from Data on Heat Transfer and Fluid Friction", Industrial and Engineering Chemistry, 26(11), pp. 1183–1187, 1934. https://doi.org/10.1021/ie50299a012

[29] Thomas, D., Vanderschuren, J. "The absorption oxidation of NOx with hydrogen peroxide for the treatment of tail gases", Chemical Engineering Science, 51(11), pp. 2649–2654, 1996. https://doi.org/10.1016/0009-2509(96)00131-5

[30] Hoftyzer, P., Kwanten, J. G. "Absorption of nitrous gases. In Gas Purification process for air pollution control", In: Nonhebel, G. (ed.) Gas Purification Processesnfor Air Pollution Control, Newnes-Butterworths, 1972, pp. 164–187. ISBN 9780408000703

[31] Thomas, D., Vanderschuren, J., Barigand, M. "Influence of acidity on the oxidation rate of nitrous acid by hydrogen peroxide", Journal de Chimie Physique et de Physico-Chimie Biologique, 95(3), pp. 523–535, 1998. https://doi.org/10.1051/jcp:1998166

[32] Lee, Y.-N., Lind, J. A. "Kinetics of aqueous phase oxidation of nitrogen (III) by hydrogen peroxide", Journal of Geophysical Research: Atmospheres, 91(D2), pp. 2793–2800, 1986. https://doi.org/10.1029/JD091iD02p02793

[33] Baveja, K. K., Subba Rao, D., Sarkar, M. K. "Kinetics of absorption of nitric oxide in hydrogen peroxide solutions", Journal of Chemical Engineering of Japan, 12(4), pp. 322–325, 1979. https://doi.org/10.1252/jcej.12.322

[34] England, C., Corcoran, W. H. "The Rate and Mechanism of the Air Oxidation of Parts-per-Million Concentrations of Nitric Oxide in the Presence of Water Vapor", Industrial & Engineering Chemistry Fundamentals, 14(1), pp. 55–63, 1975. https://doi.org/10.1021/i160053a010

[35] Holma, H., Sohlo, J. "A mathematical model of an absorption tower of nitrogen oxides in nitric acid production", Computers & Chemical Engineering, 3(1–4), pp. 135–141, 1979. https://doi.org/10.1016/0098-1354(79)80024-1

[36] Park, J. Y., Lee, Y. N. "Solubility and decomposition kinetics of nitrous acid in aqueous solution", Journal of Physical Chemistry, 92(22), pp. 6294–6302, 1988. https://doi.org/10.1021/j100333a025

[37] Corriveau, C. E. "Absorption of N_2O_3 into water", Master's thesis, Université de Berkely, 1971.

[38] Verma, P., Yang, Z., Axelbaum, R. L. "A direct contact cooler design for simultaneously recovering latent heat and capturing SO_x and NO_x from pressurized flue gas", Energy Conversion and Management, 254, 115216, 2022. https://doi.org/10.1016/j.enconman.2022.115216

[39] Aspen Technology "Aspen Plus: Getting Started Modeling Processes with Electrolytes", [pdf] Aspen Technology, Inc., Burlington, MA, USA, 2013. Available at: http://profsite.um.ac.ir/~fanaei/_private/Electrolytes%208_4.pdf [Accessed: 22 June 2023]

[40] Thomas, D. "Absorption des oxydes d'azote dans des solutions contenant des agents oxydants-Application au peroxyde d'hydrogène" (Absorption of nitrogen oxides in solutions containing oxidizing agents-Application with hydrogen peroxide), Ph.D. Thesis, Polytechnic Faculty of Mons, 1996. (in French)